



# STUDY OF COPPER CORROSION INHIBITION BY THE MINERALIZATION OF THE RED ALGA GELLIDIUM IN NITRIC ACID INVESTIGATED BY CHEMICAL AND SPECTROSCOPIC TECHNIQUES

| Bazzi Aicha <sup>1</sup> | Hilali Mustapha <sup>1</sup> | Bazzi Lahcen <sup>1</sup> | Elissami Souad <sup>1</sup> | and | Zejli Hanane <sup>1</sup> |

<sup>1</sup> Ibn Zohr University | department of chemistry | Agadir | Morocco |

| Received | 27 August 2018 | | Accepted | 07 September 2018 | | Published 20 September 2018 | | ID Article | Bazzi-ManuscriptRef.3-ajira270818 |

## ABSTRACT

**Background:** Over the past two decades, research in the field of corrosion inhibitors has been conducted with the aim of using efficient molecules with low environmental impact to replace hazardous agents likely to cause harm to the environment. Among the promising compounds that can be used as corrosion inhibitors are natural plant extracts that are environmentally friendly, non-toxic and biodegradable. **Methods:** The influence of Gellidium red algae mineralization on the inhibition of copper corrosion in 1M HNO<sub>3</sub> solutions was studied by gravimetric and electrochemical techniques (potentiodynamic polarization and electrochemical impedance spectroscopy). **Results:** The results of the interactions of the mineralized red algae with copper are supported by a qualitative follow-up using ultraviolet and quantitative concentration of copper ions by atomic absorption flame. The inhibition efficiency (IE%) has increased as the increase of the inhibitor concentration increases to reach 84%. **Conclusions:** Polarization measurements showed that the inhibitor is of cathodic type. The results obtained by means of various methods are similar.

**Keywords:** *potentiodynamic polarization, impedance spectroscopy, algae, Inhibition.*

## 1. INTRODUCTION

The present work consists in studying the degenerate effects by the interactions of certain marine plant compounds on metallic supports. The demonstration of these effects has been carried out by means of weight loss spectroscopic and electrochemical methods. An effort has been made in the present study in order to scrutinize the inhibition characteristics of some marine plant compounds on copper corrosion in a nitric acid solution. Our working matrix is a marine plant that is abundant in the Moroccan Atlantic coast and especially in El Jadida area. It is 'Gellidium', a red alga commonly known as Sésquipedal.

Our primary objective is to test mineralizer prepared by digestion of red seaweed powder (Gellidium) as inhibitor for the acidic corrosion of copper and to discuss the nature of its inhibition mechanism.

Indeed, several studies have shown that certain extracts based on natural plants are inhibitors of corrosion of metals (Cu, Fe, Zn ...) [1,2-4,5,6,7-21]. These so-called green inhibitors belong to the new generation of compounds that are not harmful to the environment [3,4]. They are biocompatible in nature and easily degradable [2,3-8]. Moreover, the judicious use of these green compounds falls within the prerogatives and the requirements imposed by the standards of the environmental protection [3,8]. They roughly replace synthetic compounds, which are expensive and harmful to the environment [9]. Naturally, inhibitors are chemical substances added to the corrosive medium in low concentrations [8] in order to reduce metal rate corrosion.

Gellidium is among the widely collected aquatic plants in Morocco. It is rich in chromophores: ethylenic groups, organic acids, alkaloids, flavonoids, terpenoids, polyphenols and tannins [4]. Several studies have shown that these compounds have a significant efficiency of corrosion inhibition [4-9-14]. Similarly, vegetable extracts contain oxochromes (nitrogen, oxygen, sulfur, etc.) [4-6-10], which are easily adsorbed on the metal surface. It's noticed that adsorbed compounds are protective barriers against any corroding attacks [14,15]. In addition, the gelidium mineralizer contains several trace metals whose ICP absorption method reveals the percentages of the constituent elements. The analysis of our results shows that the percentage relative to the copper metal is 5 .10<sup>-4</sup>%. It is therefore a metallic element in trace.

Consequently, we use copper as the metal to look for the type and nature of its interaction with the Gellidium mineralizer. In electrochemistry, we use it as a working electrode to deduce the possibility of corrosion resistance in the presence of diluted mineralization ( $\text{HNO}_3$ , 1M).

## 2. MATERIALS AND METHODS

In the methodological part, our red algae collected in El-Jadida area was dried in an oven at  $70^\circ\text{C}$  during 48 hours. It is then milled, homogenized by sieving to different dimensions. In fact, 1 g mass taps are introduced into Teflon mineralization blocks and adding 10 ml of 65% concentrated nitric acid. The set is put into a microwave oven brand Antoon Parr 3000 under the conditions of temperature of  $250^\circ\text{C}$ , 80 bar pressure and a digestion time of 40 minutes. At the end of the mineralization and after cooling, the Teflon tubes are removed from the oven and diluted with double distilled water.

Before proceeding with the study using weight loss spectroscopic and electrochemical techniques, we determined the value of  $0.077\ \mu\text{g}/\text{l}$  relative to the concentration of trace copper in the mineralization by Flame Atomic Absorption (FAA).

The results of the interactions of the mineralized red algae with copper are qualitatively monitored by UV-Visible spectrophotometry and quantitatively by Flame Atomic Absorption spectrophotometry.

For this procedure, we use a JENWAY 6800 brand scan-and-beam UV-Vis spectrophotometer driven by Flight Deck 1.0 software via R232. This qualitative technique makes it possible to highlight the type of bond formed during the interaction between the mineralizer in acidic medium and the metallic copper. We have bounded the abscissa relative to the wavelength between 190 nm and 360. The ordinate relating to the absorbance of the colorless dilute solution belongs to the interval [1, 5].

The other spectrophotometric Flame Atomic Absorption procedure is used to determine the concentration of the trace copper element before and after each mineralized metal interaction. The Flame Atomic Absorption spectrophotometer used is the brand Shimadzu AA-7000 driven by Wizaard software via the RS232 interface. The device is equipped with a non-specific background corrector (deuterium lamp), a 60-sample auto sampler and a copper hollow cathode lamp with a wavelength of 325 nm. The copper standard solutions of concentrations between 0 and  $20\ \mu\text{g}/\text{l}$  are prepared from an MBH analytical LTD brand certified parent copper solution with an initial concentration of  $999\ \mu\text{g}/\text{ml}$ .

The calibration curve is carried out using four standards with concentrations of 3, 5, 11 and  $20\ \mu\text{g}/\text{l}$ , respectively. Fig.1 gives a schematic representation of the pre-established calibration curve of absorbance as a function of the concentration of cupric ion in trace  $[\text{Cu}^{2+}]$ .

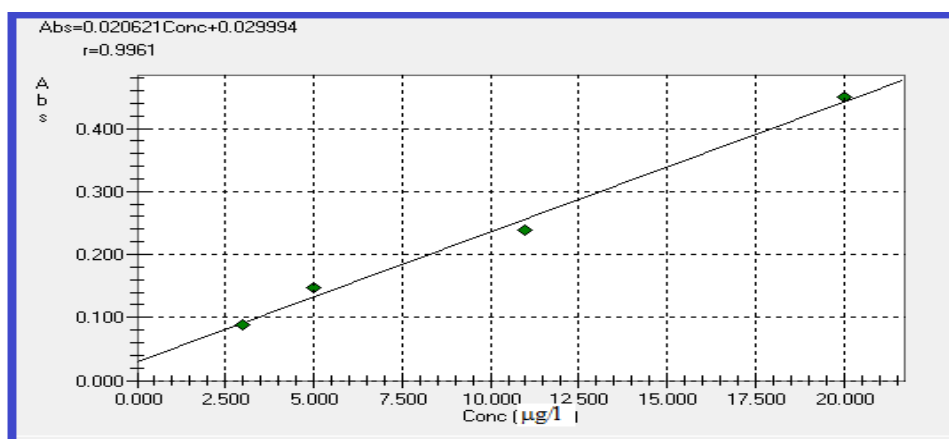


**Figure 1:** Calibration curve of the absorbance as a function of the copper concentration in trace.

The analytical expression of the linear rate of absorbance as a function of the concentration of cupric ions is reported in Fig. 1. It is a correlation line between absorbance and concentration (Beer Lambert's law) whose correlation coefficient  $R^2$  is 0.9961. From this curve, we deduce the concentration in  $\mu\text{g}/\text{l}$  samples from gravimetric and electrochemical methods.

The weight loss technique is used in this study to highlight the nature of the interaction between the acid mineralizer and the copper metal plate. In these measurements, a RADWAG 10-4g precision analytical balance is used. From this we deduce two properties: the rate of Vcor corrosion. (eq 1) and the inhibitory efficiency IE% (eq 2).

$$V_{cor} = \frac{m_1 - m_2}{At} = \frac{P}{t} \quad (\text{eq1})$$

$$IE\% = \frac{V_{cor}(\text{blank}) - V_{cor}(\text{inh})}{V_{cor}(\text{blank})} * 100 \quad (\text{eq 2})$$

Where m1 and m2 are the masses (mg) of copper coupons before and after immersion respectively in the test solutions, A is the surface of the sample (cm<sup>2</sup>) and t is the exposure time (h). Vcor. (blank) and Vor (inh) are the rate of corrosion in the absence and presence of the mineralizer at room temperature, respectively.

To do this, we immerse 36 thin copper coupons with a surface area of 1 cm<sup>2</sup> and 0.1 mm thickness in 50 ml beakers containing 10<sup>-2</sup>M of nitric acid solution (blank) and red algae mineralizers at different concentrations: 10<sup>-2</sup>, 2.10<sup>-2</sup> and 4.10<sup>-2</sup> g /l. We note that these coupons are previously polished with emery paper up to 1000 grade, rinsed thoroughly with acetone and bidistilled water.

Finally, the electrochemical technique is used to specify the mineral-metal interaction. The electrochemical measurements are performed using a VERSASTAT electrochemical device controlled by STAR software via R232. The technique contributes to the determination of the corrosion current and the inhibitory efficiency of this IE% interaction (eq.3) (eq4).

$$IE\% = \frac{I_{cor}(\text{blank}) - I_{cor}(\text{inh})}{I_{cor}(\text{blank})} * 100 \quad (\text{eq 3})$$

Where Icor (blank) and Icor (inh) are the values of the corrosion current density in blank and mineralized material.

$$IE\% = \frac{R_c(\text{inh}) - R_c(\text{blank})}{R_c(\text{inh})} * 100 \quad (\text{eq4})$$

Where Rc,inh represents the charge transfer resistance in presence of the inhibitor and Rc blank is the charge transfer resistance in blank solution. A

The experiments are carried out at a temperature of 25 ° C in a three-electrode electrochemical cell: a platinum counter-electrode (CE), a saturated calomel reference electrode and a copper-based working electrode.

Prior to the electrochemical measurements, the copper working electrode was immersed in open potential test solution (OCP) for 20 min to reach a stable state. The potential of the polarization curves was initiated from -0.8V to 0.4V at a scanning rate of 0.01 mV.

Parallel to this, electrochemical impedance spectroscopy (EIS) was performed at OCP in the frequency range between 0.01Hz to 100000 Hz under a voltage of 10 mV. It determines the mechanism at the metal solution surface.

Finally, we use the software Origin '10' for the graphic processing of the results obtained during this study.

### 3. RESULTS AND DISCUSSION

#### 1. Determination of Optimum mineralization concentration by UV-Visible spectrophotometry:

We start by optimizing the initial concentration of our mineralizer in UV-Visible spectrophotometry. Indeed the validation of the law of Beer LAMBEERT lies on the use of the diluted solutions of the mineralizer powder of the red algae. By varying the concentration between 10<sup>-1</sup> and 10<sup>-5</sup> M, we deduce their UV-Visible spectrum whose wavelength varies between 190 and 350 nm (see Fig. 2).

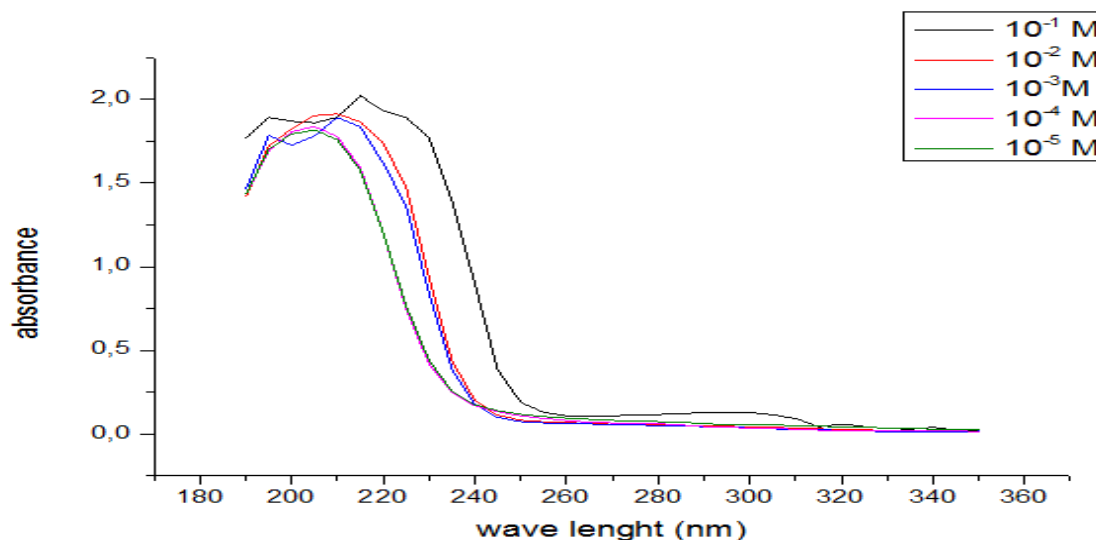


**Figure 2:** Variation of the absorbance  $A$  as a function of the wavelength  $\lambda$  of the different solutions of the mineralizer.

The characteristic UV-Visible spectrum of the mineralizer becomes significant when the equality of the Beer-LAMBEERT law is reached. By analyzing these spectra above, we report in Table1, the coordinates at the maximum ( $\lambda_{max}$ ,  $A_{max}$ ) of each concentration of the mineralizer.

**Table 1:** Values of the coordinates ( $\lambda_{max}$ ,  $A_{max}$ ) of the different mineralization solutions

Solution	$10^{-1} M$	$10^{-2} M$	$10^{-3} M$	$10^{-4} M$	$10^{-5} M$
$\lambda_{max}$	220	215	216	215	215
Absorbance	2.022	1.892	1.738	1.663	1.598

We note for a concentration  $10^{-1} M$ , an appearance of a wide band whose coordinates at maximum are equal to ( $\lambda_{max} = 220nm$ ,  $A_{max} = 2.022$ ). At  $10^{-2} M$ . We observe a hypochromic effect ( $\lambda_{max} = 215 nm$ ,  $A = 2.022$ ) which results in the decrease of the absorbance to a value of  $A_{max} = 1.892$ . We call this solution optimal because its spectrum has an acute band and a gaussian-like appearance. And if we continue to decrease the concentration, we notice a clearly visible hypochromic effect and also a hypochromic effect.

This optimal concentration of  $10^{-2} M$  will be used only in the gravimetric part to determine the nature of the interaction between the red algae mineralizer and the metallic copper.

## 2. Gravimetric study of mineralization and metallic copper

In this part, we will study the effects due to the influence of the interaction resulting from the immersion of the copper plate on the mineralizer. We notice changes on the metal and then at the solid-liquid interface within the solution.

### 2.1. Study of the solid

By applying the specific gravimetric procedure, we summarize in Table 2 the results relating to the mass losses of the 36 copper plates. These are the average gravimetric values corresponding to the three concentrations close to the optimum concentration:  $10^{-2} g / l$ ,  $2 \cdot 10^{-2} g / l$  and  $4 \cdot 10^{-2} g / l$  of the mineralizer at the different immersion times: 30, 60 and 90 minutes.

**Table 2:** Gravimetric results relating to the losses of mass of the copper plates

	Perte de masse 30 min (mg / cm <sup>2</sup> )	60min	90min	
$10^{-2} g / l$	<b>Pblanc</b>	1.0000	1.2000	1.3300
	<b>Pcorrosion</b>	0.1997	0.2000	0.4660
$2 \cdot 10^{-2} g / l$	<b>Pblanc</b>	0.9000	1.0000	1.0600
	<b>Pcorrosion</b>	0.1333	0.2399	0.3330
$4 \cdot 10^{-2} g / l$	<b>Pblanc</b>	1.2000	1.1800	1.6600
	<b>Pcorrosion</b>	0.1300	0.2000	0.2000

We conclude that the loss of mass in the surface area of copper depends on two variables: time (t in min) and concentration (C in g / l). Figures 3 and 4 below give a graphical presentation of the mass losses from Table 2.

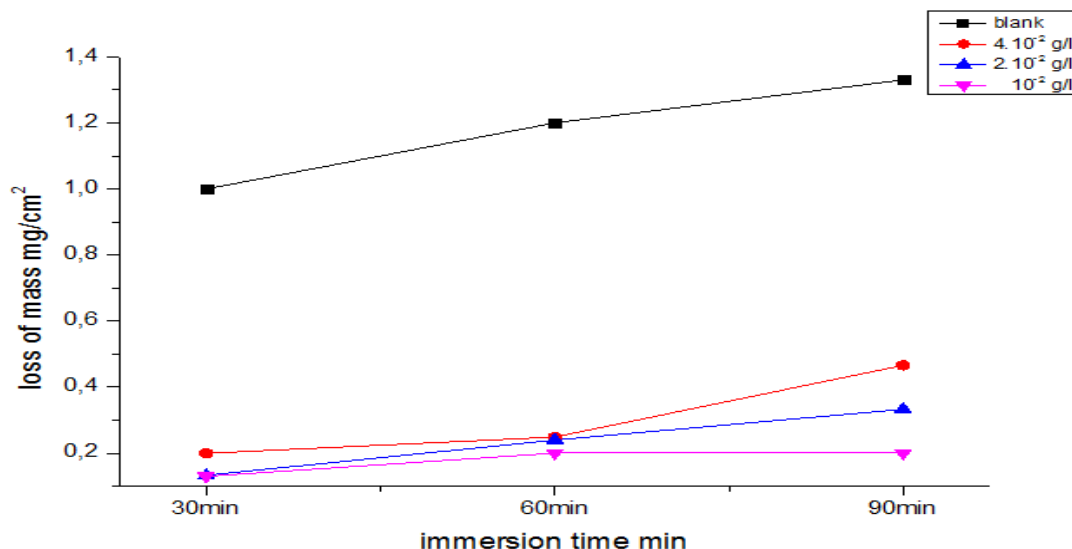


**Figure3:** Variation of the loss of mass P as a function of the time (in min) in the absence and in the presence of the mineralizer.

In Fig. 3, we observe whatever the concentration of the mineralizer, the loss of mass increases with time and it remains lower compared to blank solution. In addition, in Fig. 4 below, we conclude that the increase in the concentration of the mineralizer leads to a decrease in mass loss compared to the blank solution.

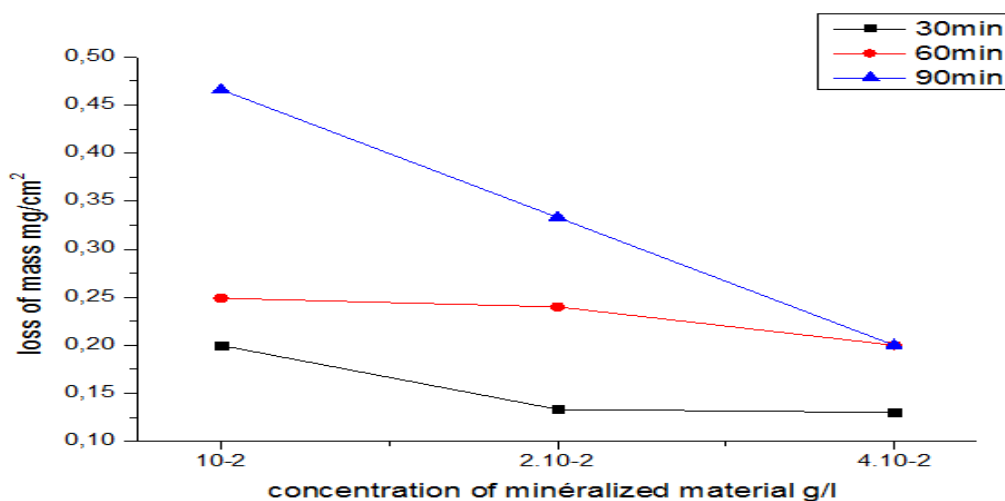


**Figure 4:** Variation of the weight loss P as a function of the concentration (g/l) in the absence and in the presence of the mineralizer.

## 2.2. Effect at the solid-liquid interface

The measurement of the effect of the interaction between the metal plate and the mineralization solution is calculated by means of the corrosion rate  $R_{cor}$  (Eq 1). Table 3 shows the rate of corrosion and the inhibitory efficiency  $IE\%$  of  $10^{-2}M$  nitric acid (blank) and the different concentrations of the mineralizer.

**Table 3:** Corrosion rate percentage of the inhibition efficiency.

	30min		60 min		90 min	
	Rcor. mg / cm <sup>2</sup> .h	IE%	Rcor.mg / Cm2 .h	IE%	Rcor.mg / Cm2 .h	IE%
0 g / l	2	-	1.2	-	1.11	-
10 <sup>-2</sup> g / l	0.3994	80.03	0.2	83.33	0.31	72.77
2.10 <sup>-2</sup> g / l	0.2666	86.7	0.23	81.48	0.22	80.18
4.10 <sup>-2</sup> g / l	0.26	86,33	0.2	83,33	0.13	88,28

From the results below, we observe that whatever the immersion time is, the corrosion rate of the blank is always higher than that of the solution containing the mineralizer. This is a phenomenon of inhibition (reference book). As a result, the interface mechanism (adsorption, VDW bonding) leads to the formation of a layer of mineralized material deposited on the surface of the copper. From Table 3 the percentage of the inhibition efficiency increases with the concentration of the mineralizer and reaches a maximum of 88.28% after 90 minutes at a concentration of  $4 \cdot 10^{-2}$  g/l of the mineralizer. This result is close to the percentages obtained by other research that we have collected in Table No. 4.

**Table 4:** Percentage of the inhibition efficiency of certain natural extracts on different metals.

Plant vegetal	Métal	Midium	IE%	Autor
marine microalgae	mild steel	aluminum alloy	83.23	Wan Nik 2012 [13]
Gracilaria bursa-pastoris	mild steel	HCl	91	Ramdani 2015 [11]
Caulerpa prolifera	mild steel	HCl	96.34	Ramdani 2015 [12]
Red algae Gellidium	copper	HNO3	88.28	The present work

To explain this inhibition, we performed a chemical analysis by inductively coupled plasma spectroscopy (ICP) of the Gellidium powder. The results given in Table 5 make it possible to identify the chemical composition of our red algae.

**Table 5:** Percentage of some elements in the powder of the red alga Gelidium.

Ag	Cu	Fe	K	Mg	Mn	Na	Zn
0.0008	0.0005	0.0592	2.34	0.66	0.0031	1.64	0.011
Al	As	Ca	Co	Li	Ni	Sn	Si
0.0281	0.0006	0.4	0.0001	<0.0001	0.0006	0.0001	<0.0001

The results reveal high percentages corresponding to potassium ions  $K^+$  (2.34%) and sodium  $Na^+$  (1.64%). For the nitrate mineralizer, we have in addition positive ions, the formation in solution of  $NO_3^-$  negative ions in abundance. In fact, copper is a metal whose  $Cu^{2+}$  cupric positive ions are embedded in an electron field. It forms ABAB planes whose mesh is cubic with centered faces. We notice two types of simultaneous Coulomb electrostatic interactions. The first type is caused by the positive ions  $K^+$  (2.34%) and  $Na^+$  (1.64%) of the mineralizer, which migrate near the metal surface and enter into attraction with the electrons of the metal network. The second type of interaction is caused by the  $NO_3^-$  negative ions that enter into Coulomb attraction with  $Cu^{2+}$  cupric ions (or Cu (II)) and form metal bonds at the interface [22].

In addition, the weight loss resulting from the dissolution of the cupric ions causes the formation of porous gaps on the surface of the metal plate. This allows the positive ions of the mineralizer to eventually be lodged on the lacunary pores. There are other interactions at the solid liquid interface that cause a decrease in the rate of corrosion. Clogging of the copper metal surface is another factor that is responsible for the decrease in  $V_{cor}$ .

At the macroscopic scale, we observe a dark greenish coloration corresponding to the formation of a protective monolayer on the surface of the metal plate. Umoren was able to show that the molecular structure of the inhibitor plays a dominant role in the interactions between the inhibitor and the surface of the metal [16].

### 2.3. Effect on the solution

atomic flame absorption

We note that the oxidation of metallic copper contributes to the production of  $Cu^{2+}$  cupric ions according to the reaction below:



The Flame Atomic Absorption method quantitatively determines the concentration of trace cupric ions in the solution. We have put them into groups in the Table 6.

**Table 6:** Concentrations of cupric ions in solution by AAF.

[ minéralisât ] g / l	[Cu <sup>2+</sup> ] µg / l				
	10min	20min	30min	60min	90min
10 <sup>-2</sup>	73.6431	69.9090	0.8635	0	0
2.10 <sup>-2</sup>	43.4750	18.2340	1.8635	0	0
4.10 <sup>-2</sup>	30.8812	33.4999	0.9765	0	0

From this table, we conclude that the concentration of cupric ions  $[Cu^{2+}]$  decreases with the increase of the immersion time of the metallic copper in the mineralizer. This decrease can be explained by the phenomenon of complexation of cupric  $Cu^{2+}$  ions with  $NO_3^-$  anions of acid mineralization. In atomic flame absorption, the copper complexes evaporate as the temperature increases gradually. In addition the zero value relative to  $[Cu^{2+}]$  is detected in our calibration range. Moreover, the UV-Visible qualitative method highlights the  $Cu(NO_3)_2$  complex at 300 nm. Fig. 5 shows graphically by origin the spectra of the mineralizer alone, the gravimetric solution of nitric acid and the three gravimetric solutions of the mineralizer.

UV-Visible spectrophotometry

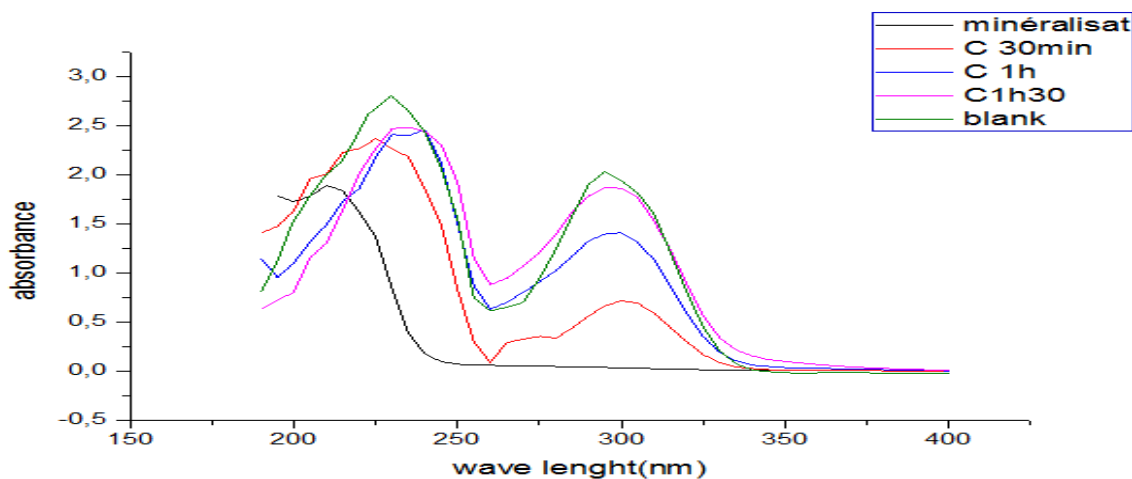


**Figure 5:** Ultraviolet spectra of the solutions of the gravimetry in the absence and in the presence of the mineralizer ( $4 \cdot 10^{-2}$  g/l) at different immersion time.

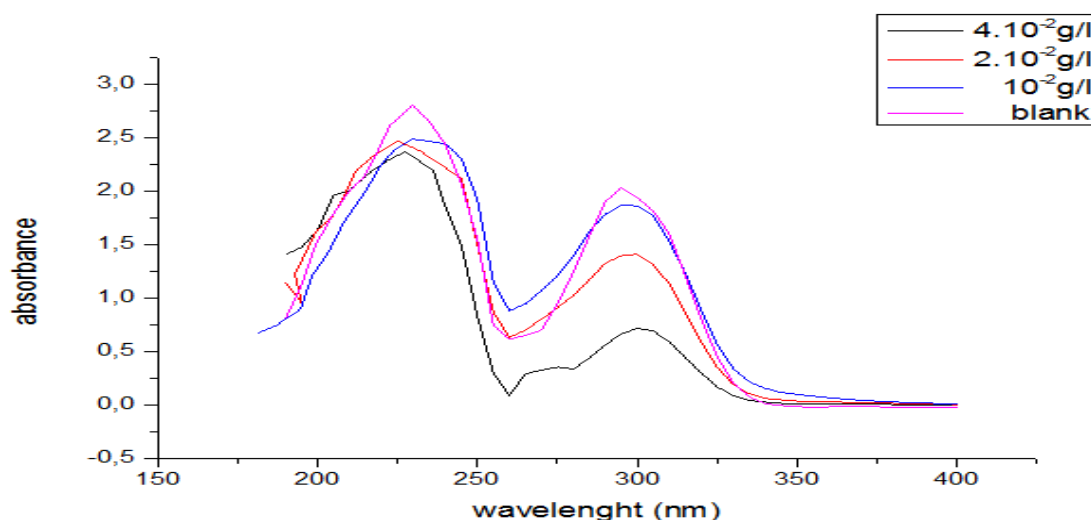


**Figure6:** ultraviolet spectrum of gravimetric solutions for different concentrations of mineralizer.

The analysis of curves presented in Fig. 5 leads to several conclusions : the solution of the mineralizer alone shows the existence of a single peak unlike the solutions of the mineralists after immersion of the copper plates. Indeed, in these solutions, the appearance of a second peak (around 270 nm) is observed. This peak corresponds to the copper ions resulting from the dissolution of the copper plate in the acidic medium. However, a marked decrease in Absorbance between the media containing the mineralizer versus solutions containing nitric acid alone. This decrease in absorbance corresponds to a decrease in the concentration of the copper ions resulting from the dissolution of the copper plate. This concentration tends to decrease by increasing the concentration of the mineralizer. This is confirmed in Figure 6, which shows the ultraviolet spectrum of gravimetric solutions for different concentrations of mineralizer and white.

Indeed, in Figure 6 we notice a hypochromic effect, a decrease in the intensity of absorption due to the influence of the concentration of the mineralizer, the concentration of copper ions decreases therefore by increasing the concentration of the mineralizer of  $10^{-2}$  to  $4 \cdot 10^{-2}$  g / l.



### 3. Electrochemical study

Electrochemical methods are among the most commonly used techniques for determining the rate of corrosion, its main use is the plot of polarization curves, in addition to the Verasastat program allows the logarithmic current to be plotted and the use of Tafel's method makes it possible to determine the value of the corrosion current and other electrochemical parameters.

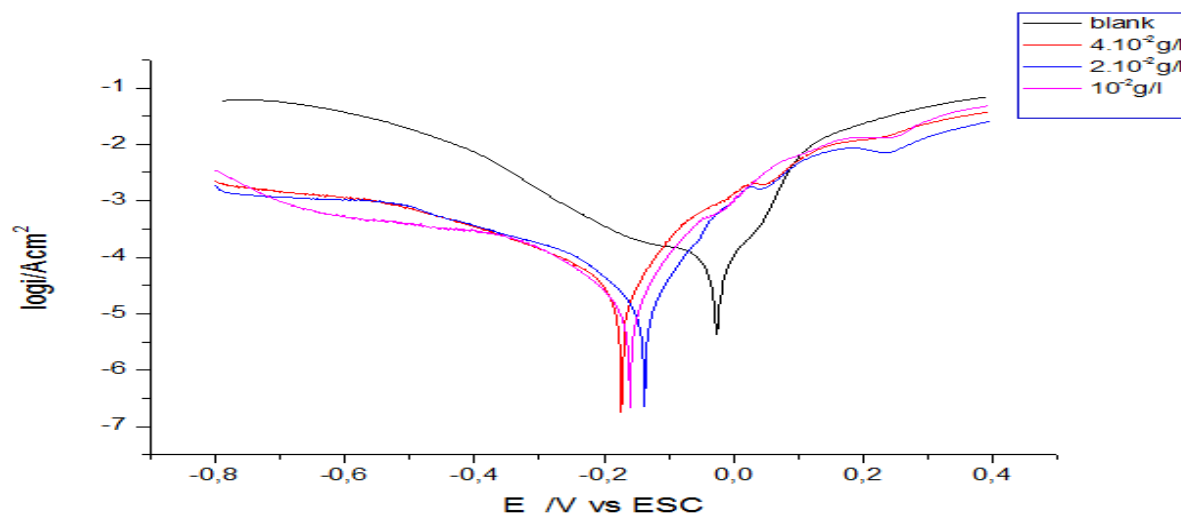


**Figure9.** Tafel polarization curves for copper at various concentrations of red algae mineralizer in 1 M HNO<sub>3</sub>.

The behaviour of copper against polarization of the surface in 1M HNO<sub>3</sub> with different concentrations of red algae mineralizer in 25°C is shown in Fig. 9.

The difference between the shape of the blank curve and that obtained during the addition of the mineralizer can be attributed to a change in the mechanism of corrosion [17].

It is difficult to determine the linear region at the cathodic portion, this may be due to the diffusion mechanism at the oxygen reduction level, on the contrary a typical linear region is observed at the anodic portion from which the current density ( $i_{corr}$ ) and the potential for corrosion  $E_{corr}$  can be determined by extrapolation.

The electrochemical parameters of corrosion such as corrosion current density  $i_{corr}$  which calculated with the extrapolation of the linear parts of Tafel lines to  $E_{corr}$ , corrosion potential  $E_{corr}$ , anodic Tafel constants  $B_a$  and inhibition efficiency  $IE\%$  were calculated from the polarization curves and presented in Table 7.

**Table7:** Electrochemical kinetic parameters, inhibition efficiencies (%IE) for copper in 1 M HNO<sub>3</sub> solutions without and with various concentrations of red algae mineralizer at 25 ± 1 °C.

	$i_{corr}$ Acm <sup>-2</sup>	$E_{corr}$ V vs SCE	$B_a$ mV dec <sup>-1</sup>	%IE
Blank	7.085 10 <sup>-5</sup>	-0.0236	55.79	–
10 <sup>-2</sup> g/l	1.30 10 <sup>-5</sup>	0.1624	58.82	81.65%
2.10 <sup>-2</sup> g/l	1.20 10 <sup>-5</sup>	0.1624	74.53	83.06%
4.10 <sup>-2</sup> g/l	8.550 10 <sup>-6</sup>	-0.1743	75.68	87.93%

After the addition of the inhibitor  $B_a$  doesn't vary, indicating that the dissolution of the copper is blocked. The addition of the mineralizer may also decrease the current density. The addition of the inhibitor promotes the decrease of the cathodic current density these remarks indicate that the impact of the inhibitor is accentuated at the level of the cathodic reduction than the level of the anodic dissolution. Thus, addition of this inhibitor reduces the hydrogen evolution reaction. The corrosion current density was found to decrease in the presence of the inhibitors accompanied by an increase of the inhibition efficiency values.

Electrochemical Impedance Spectroscopy (EIS) is a well-established and powerful technique in the study of corrosion. The properties of the surface, the kinetics of the electrodes and the mechanical information can be obtained from the impedance diagrams [19].



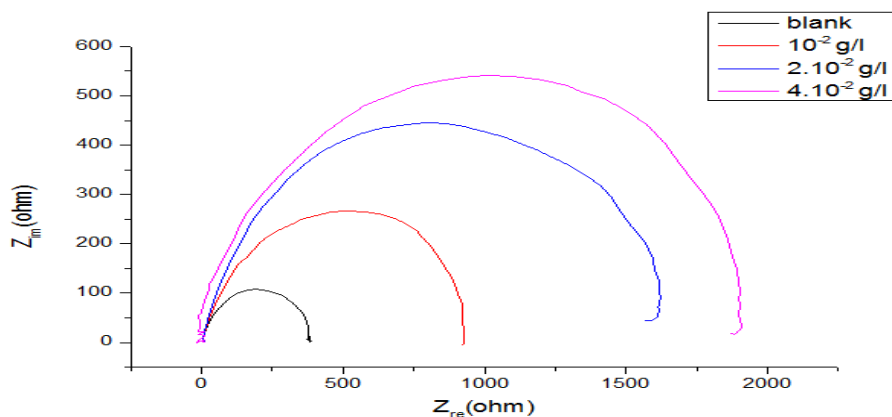


**Figure 6:** Nyquist plot at different concentrations of red algae mineralizer in 1M HNO<sub>3</sub> solution.

The corrosion behavior of copper in 1 M HNO<sub>3</sub> solution with and without the inhibitor was investigated by EIS measurements. Fig. 11 shows all the impedance spectra in the absence and presence of red algae mineralizer with different concentrations in the form. The diameter of the semicircle was increased with increasing inhibitor concentration. Nyquist plots do not present perfect semi-circles; they show a depressed capacitive loop in the high frequency range. The deviation of the perfect circular shape of the half cycles can be attributed to the roughness and the inhomogeneity of the surface of the electrode [17,18].

**Table 8:** Impedance parameters copper in 1M HNO<sub>3</sub> in the absence and presence of different concentrations of Gellidium mineralizer.

	$R_s(\text{ohm.cm}^2)$	$R_t(\text{ohm.cm}^2)$	$CPE(\mu\text{F.cm}^{-2})$	%IE
Blank	0.8677	9.163	$8.594 \cdot 10^{-5}$	0
$10^{-2} \text{ g/l}$	0.9670	11.60	$7.232 \cdot 10^{-5}$	71.03
$2 \cdot 10^{-2} \text{ g/l}$	0.9144	16.53	$3.649 \cdot 10^{-5}$	78.58
$4 \cdot 10^{-2} \text{ g/l}$	0.7697	25.62	$4.490 \cdot 10^{-5}$	81.24

According to the Table 8, the value of  $R_T$  Transfer resistance increases by increasing the concentration of Gellidium mineralization, this confirms that it is the charge transfer mechanism which controls the corrosion of copper in nitric acid and subsequently there is an increase in inhibitory efficiency % IE. Decrease in the CPE double capacity layer was caused by reduction in local dielectric constant [17,18-21].

## CONCLUSION

The inhibitory efficacy of the mineralization of the red alga Gellidium against copper in nitric acid was studied using gravimetric, spectroscopic and electrochemical techniques. This study resulted in a set of results:

For the gravimetric part we notice modifications on the metal then at the solid-liquid interface and also in the solution. Indeed, we note for the metal that, whatever the concentration is, the mass loss of the mineralizer increases with time and remains always lower compared to white, concerning the solid interface -liquide the corrosion rate of the white is always greater than that of the solution containing the mineralizer for different immersion times. This is a phenomenon of inhibition.

Within the solution, the flame atomic absorption method quantitatively determines the concentration of cupric ions in trace. The latter decreases during the increase of the immersion time of the metallic copper in the mineralizer. This decrease can be explained by the phenomenon of complexation of cupric  $\text{Cu}^{2+}$  ions with  $\text{NO}_3^-$  anions of acid mineralization. The results of electrochemical tests reveal that the corrosion current decreases after addition of inhibitor in the HNO<sub>3</sub> solution and the inhibitory efficiency increases with the increase of the concentration of the mineralizer and reaches a value equal to 87.93%. The trend of the polarization curves suggested that the addition of the inhibitor in a small amount to the nitric acid solution shifted the curves to the region of the lower current in the cathodic potential direction, relative to the white acid solution.

Therefore, the addition of red algae mineralization has influenced the cathodic reactions that could be visualized via changes in the shape of the Tafel polarization curves. Actually, it effectively reduces the cathodic current density, indicating that the mineralized material red algae act as a cathodic-type inhibitor.

The impedance curves were approximated by unique capacitive semicircles, showing that the corrosion process was mainly charge transfer. The general shape of the curves is very similar for all concentrations (in the presence or absence of inhibitor) indicating that there is no change in the mechanism of corrosion.

## 6. REFERENCES

1. Shi M., Ling J., Hong Q., Nian B. An example of green copper corrosion inhibitors derived from flavor and medicine: Vanillin and isoniazid. *Journal of Molecular Liquids*. 2017; 242:822–830.
2. Deyab M.A., Egyptian licorice extract as a green corrosion inhibitor for copper in hydrochloric acid solution. *Journal of Industrial and Engineering Chemistry*. 2015; 22:384–389.
3. Golestani Gh., Shahidi M., Ghazanfari D. Electrochemical evaluation of antibacterial drugs as environment-friendly inhibitors for corrosion of carbon steel in HCl solution. *Applied Surface Science*. 2014; 308: 347–362.
4. Manimegalai S., Manjula P. Thermodynamic and Adsorption studies for corrosion Inhibition of Mild steel in Aqueous Media by Sargassum swartzii (Brown algae) . *Journal of material environmental Science*. 2015; 6: 1629-1637.
5. Zaabar A., Aitout R., Makhoulfi L., Alilat K., Maziz S., Saidani B. Effect of nettle plant extract on the cementation of copper onto zinc in acidic sulfate solutions. *Environmental Science*. 2015; 6:1629-1637.
6. Abdel-Gaber A.M., Abd-El-Nabey B.A., Sidahmed I.M., El-Zayady A.M., Saadawy M. Inhibitive action of some plant extracts on the corrosion of steel in acidic media. *Corrosion Science*. 2006; 48 : 2765–2779.
7. Krishnaveni K., Ravichandran J. Influence of aqueous extract of leaves of Morinda tinctoria on copper corrosion in HCl medium. *Journal of Electroanalytical Chemistry*. 2014; 735: 24–31.
8. Ehsani A., Mahjani M.G., Hosseini M., Safari R., Moshrefi R., Mohammad Shiri H. Evaluation of Thymus vulgaris plant extract as an eco-friendly corrosion inhibitor for stainless steel 304 in acidic solution by means of electrochemical impedance spectroscopy, electrochemical noise analysis and density functional theory. *Journal of Colloid and Interface Science*. 2017; 490:444–451.
9. Rahal C., Masmoudi M., Abdelhedi R., Sabot R., Jeannin M., Bouaziz M., Refait P. Olive leaf extract as natural corrosion inhibitor for pure copper in 0.5 M NaCl solution: A study by voltammetry around OCP. *Journal of Electroanalytical Chemistry*. 2016; 769 :53–61.
10. Parthipan P., Narenkumar J., Elumalai P., Sujatha P., Ayyakkannu P., Nanthini U., Agrawal A., Rajasekar A. Neem extract as a green inhibitor for microbiologically influenced corrosion of carbon steel API 5LX in a hypersaline environments. *Journal of Molecular Liquids*. 2017; 240: 121–127.
11. Ramdani M., Elmsellem H., Haloui B., Ramdani M., Elkhiahi N., Layachi M., Mesfioui A., Hammouti B., Aouniti A. and El Mahi B. Gracilaria bursa-pastoris as eco-friendly corrosion inhibitor for mild steel in 1 M HCl media. *Der Pharma Chemica*. 2016; 8:300-337.
12. Ramdani M., Elmsellem H., Elkhiahi N., Haloui B., Aouniti A., Ramdani M., Ghazi Z., Chetouani A., Hammouti B. Caulerpa prolifera green algae using as eco-friendly corrosion inhibitor for mild steel in 1 M HCl media. *Der Pharma Chemica*, (2015),7: 67-76.
13. Wan Nik WB., Sulaiman O., Ayob AF., Ahmad MF., Rahman MM. Marine Extracts as Corrosion Inhibitor for Aluminum in Seawater Applications. *International Journal of Engineering Research and Applications*. 2012 ,2 : 455- 458.
14. Lebrini M., Robert F., Lecante A., Roos C. Corrosion inhibition of C38 steel in 1 M hydrochloric acid medium by alkaloids extract from Oxandra asbeckii plant. *Corrosion Science*. 2011; 53: 687–695.
15. Ramde T., Rossib S., Zanella C. Caterina Zanella Inhibition of the Cu65/Zn35 brass corrosion by natural extract of Camellia sinensis Tambi. *Applied Surface Science*. 2014; 307:209–216.
16. Jmiai A., El Ibrahim B., Tara A., Oukhrib R., El Issami S., Jbara O., Bazzi L., Hilali M. Chitosan as an eco-friendly inhibitor for copper corrosion in acidic medium: protocol and characterization. *Cellulose* 10.1007/s10570-017-1381-2017.
17. Karthik G., Sundaravidvelu M. Investigations of the inhibition of copper corrosion in nitric acid solutions by levetiracetam drug. *Egyptian Journal of Petroleum*. 2016; 25:481–493.
18. Ashassi-Sorkhabi H., Seifzadeh D., Hosseini M.G. EN, EIS and polarization studies to evaluate the inhibition effect of 3H-phenothiazin-3-one, 7-dimethylamin on mild steel corrosion in 1 M HCl solution. *Corrosion Science*. 2008; 50: 3363–3370.
19. Fouda A.S., Wahed H.A. Corrosion inhibition of copper in HNO<sub>3</sub> solution using thiophene and its derivatives. *Arabian Journal of Chemistry*. 2016; 9: 91–99.
20. Rekkab S., Zarrok H., Salghi R., Zarrouk A., Bazzi Lh., Hammouti B., Kabouche Z., Touzani R., Zougagh M. Green Corrosion Inhibitor from Essential Oil of Eucalyptus globulus (Myrtaceae) for C38 Steel in Sulfuric Acid Solution. *Journal of Material and Environmental Science*. 2012; 3(4): 613-627.
21. Umoren S.A., Eduok U.M., Solomon M.M., Udoh A.P. Corrosion inhibition by leaves and stem extracts of Sida acuta for mild steel in 1 M H<sub>2</sub>SO<sub>4</sub> solutions investigated by chemical and spectroscopic techniques. *Arabian Journal of Chemistry*. 2016; 9:209–224.
22. Milic S.M., Antonijevic M.M. Some aspects of copper corrosion in presence of benzotriazole and chloride ions. *Corrosion Science*. 2009 ;51: 28–34.



**Cite this article: Bazzi Aicha, Hilali Mustapha, Bazzi Lahcen, Elissami Souad, and Zejli Hanane.** STUDY OF COPPER CORROSION INHIBITION BY THE MINERALIZATION OF THE RED ALGA GELLIDIUM IN NITRIC ACID. *Am. J. innov. res. appl. sci.* 2018; 7(3): 159-168.

This is an Open Access article distributed in accordance with the Creative Commons Attribution Non Commercial (CC BY-NC 4.0) license, which permits others to distribute, remix, adapt, build upon this work non-commercially, and license their derivative works on different terms, provided the original work is properly cited and the use is non-commercial. See: <http://creativecommons.org/licenses/by-nc/4.0/>